Free-boundary, non-stellarator-symmetric calculations using the Stepped Pressure Equilibrium Code

S. R. Hudson
Princeton Plasma Physics Laboratory, PO Box 451, Princeton NJ 08543, USA

C. Zhu
University of Science and Technology of China, 96 JinZhai Road, Hefei, Anhui 230026, P. R. China

J. Loizu
Max-Planck-Institut für Plasmaphysik, D-17491 Greifswald, Germany

S. Lazerson
Princeton Plasma Physics Laboratory, P.O. Box 451, Princeton NJ 08543, USA
(Dated: March 4, 2018)

Free-boundary, non-stellarator-symmetric calculations using the Stepped Pressure Equilibrium Code (SPEC) are described. It is verified that SPEC is correctly computing the "vacuum" field produced by a set of external, current-carrying loops as calculated using the Biot-Savart rule.

A. Introduction

The Stepped Pressure Equilibrium Code (SPEC) is based on the multi-region relaxed magnetohydrodynamic (MRxMHD) equilibrium model introduced by Dewar and co-workers [1–3]. This model was motivated, in part, by the results of Bruno & Laurence [4], who presented theorems guaranteeing the existence of well-defined, stepped-pressure solutions to the MHD equilibrium equations in three-dimensional (3D) geometry provided certain conditions reminiscent of the Kolmogorov-Arnold-Moser (KAM) theorem [5, 6] are satisfied.

Dennis *et al.* have presented generalizations of MRxMHD that include flow [7] and pressure anisotropy [8]; and Lingam *et al.* [9] have presented a model of multi-region relaxed Hall MHD. The static equilibrium model has recently been extended to a fully dynamical model by Dewar *et al.* [10]. A generalization of MRxMHD that accommodates globally continuous and smooth equilibria, with magnetic islands and chaos, in 3D geometry has been described by Hudson & Kraus [11].

The algorithm and numerical details of SPEC are described by Hudson *et al.* [12]. SPEC was used by Dennis *et al.* [13] to investigate the formation of the single-helical and double-helical states in a reversed field pinch; and by Loizu *et al.* [14] to compute the pressure-driven $1/x$ and the δ-function singular current-densities in ideal-MHD equilibria with resonantly perturbed boundaries (this required taking the "ideal limit", in which MRxMHD reduces to ideal MHD [15]). A linearized version of SPEC and the full nonlinear version were verified against analytic calculations of resonant magnetic perturbation penetration in cylindrical geometry by Loizu *et al.* [16, 17]. Fixed-boundary, vacuum SPEC calculations in strongly shaped stellarator geometries were verified [18] against a Biot-Savart code.

This paper presents the first free-boundary calculations using SPEC . The outline of this paper is as follows. First, a brief description of MRxMHD is presented. Then, the numerical discretization employed by SPEC and various recent code modifications are described. These include: using Chebyshev polynomials to represent the radial dependence of the Fourier harmonics of the vector potential; the inclusion of the non-"stellarator-symmetric" terms, so that equilibria with arbitrary geometries can be computed; the augmentation of the fixed-boundary calculation with a vacuum field solver; and the implementation of a virtual-casing method for calculating the magnetic field produced by the plasma currents at a location external to the plasma. Free-boundary equilibrium states can now be computed. Some example calculations are then presented.

B. MRxMHD

The classic MHD energy functional [19] is given by

$$W \equiv \int_{\mathcal{V}} \left(\frac{p}{\gamma - 1} + \frac{B^2}{2} \right) dv, \tag{1}$$

where $\mathcal{V}$ is the plasma volume, which is bounded by a surface, $\partial\mathcal{V}$, to which the magnetic field is assumed to be tangential.

Restricting attention to ideal variations in the pressure, $\delta p = (\gamma - 1)\,\boldsymbol{\xi} \cdot \nabla p - \gamma \nabla \cdot (p\,\boldsymbol{\xi})$, and magnetic field, $\delta \mathbf{B} = \nabla \times (\boldsymbol{\xi} \times \mathbf{B})$, the first order variation in W induced by a plasma displacement, $\boldsymbol{\xi}$, assumed to vanish at the plasma boundary, is given by

$$\delta W \equiv \int_{\mathcal{V}} (\nabla p - \mathbf{j} \times \mathbf{B}) \cdot \boldsymbol{\xi}\, dv. \tag{2}$$

Extremizing solutions, i.e., fixed-boundary, ideal-MHD equilibria, satisfy the ideal force-balance condition, $\nabla p = \mathbf{j} \times \mathbf{B}$.

Ideal variations constrain the topology of structures traced out by the magnetic fieldlines. Multi-region, relaxed MHD (MRxMHD) allows for a less-restrictive class of variations; variations that allow the magnetic field to "tear" and for magnetic islands and chaotic fieldlines to emerge. Some constraints are included to avoid "globally relaxed" solutions.

The "relaxed" aspect of MRxMHD follows the ideas under-pinning Taylor relaxation [20], namely that weakly resistive plasmas will dynamically evolve to minimize the energy under the constraint that the helicity,

$$K \equiv \int_{\mathcal{V}} \mathbf{A}\cdot\mathbf{B}\, dv, \tag{3}$$

is conserved [21, 22], where $\mathbf{B} = \nabla\times\mathbf{A}$. Mathematically, solutions are constructed by finding the minimum of the function W subject to the constraint $K = K_0$, which are identified as extrema of $\mathcal{F} \equiv W - \mu(K - K_0)/2$, where μ is a Lagrange multiplier, and the factor of $1/2$ is introduced for convenience. Allowing for unrestricted variations in $\mathbf{A}$, and with the only constraint on the pressure being $pV^\gamma = P$, where V is the volume of $\mathcal{V}$ and P is a constant, magnetic fields that extremize $\mathcal{F}$ satisfy the Beltrami equation, namely $\nabla\times\mathbf{B} = \mu\mathbf{B}$, and the pressure is constant, $p = P/V^\gamma$.

The "multi-region" aspect of MRxMHD is to partition the plasma volume into a finite number, N_V, of subregions, $\mathcal{V}_v$, which are separated by a set of nested interfaces, $\mathcal{I}_v$, for $v = 1,\ldots,N_V$ with $\mathcal{I}_{N_V} = \partial\mathcal{V}$, that are "ideally constrained" to remain intact during the minimization and therefore constitute barriers that frustrate global relaxation.

The MRxMHD energy principle is to minimize the plasma energy subject to the constraints of conserved helicity in *each* of the $\mathcal{V}_v$. This is represented mathematically as finding extrema of

$$\mathcal{F} = \sum_{v=1}^{N_V} \left[W_v - \mu_v\left(K_v - K_{v,o}\right)/2\right], \tag{4}$$

where W_v and K_v are the energy and helicity integrals, as given in Eqn. 1 and Eqn. 3 but restricted to the v-th region.

The magnetic field is constrained to remain tangential to the $\mathcal{I}_v$, but within each volume the topology of the field is unconstrained. (In the limit $N_v \to \infty$ of infinitely many ideal interfaces [15], the topology is constrained everywhere.)

The constraint on the pressure is $p_v V_v^\gamma = P_v$. The internal energy in $\mathcal{V}_v$ is $\int_{\mathcal{V}_v} p_v/(\gamma-1)\, dv = P_v V_v^{(1-\gamma)}/(\gamma-1)$, and the first variation of this due to a deformation, $\boldsymbol{\xi}$, of the ideal interfaces is $-p\int_{\partial\mathcal{V}_v}\boldsymbol{\xi}\cdot d\mathbf{s}$. Constraints on the enclosed toroidal and poloidal fluxes in each volume, $\Delta\psi_{t,v}$ and $\Delta\psi_{p,v}$, must also be included.

The Euler-Lagrange equations for extremizing states allowing for variations in the magnetic vector potential in each region and for variations in the geometry of the ideal interfaces are: (i) in each $\mathcal{V}_v$ the magnetic field is a linear force-free field, $\nabla\times\mathbf{B} = \mu_v\mathbf{B}$; and (ii) across each of the $\mathcal{I}_v$, the total pressure is continuous, $[[p + B^2/2]] = 0$. To avoid a problem of small-divisors, the rotational-transform on the ideal interfaces are generally required to be strongly irrational [4, 12, 23]. Such equilibria are called stepped-pressure states.

In each region, given the geometry of the adjacent interfaces, there are three parameters that define the solution for the magnetic field, namely the enclosed toroidal and poloidal fluxes, $\Delta\psi_{t,v}$ and $\Delta\psi_{p,v}$, and the required helicity, $K_{o,v}$. (This paper shall leave the question of bifurcations to future work.) As is typical for using Lagrange multipliers, the value of the helicity multiplier, μ_v, must be adjusted to enforce the helicity constraint; and the appropriate value of μ_v is only known *a posteori*.

Alternatively, it is possible, in some cases, to instead constrain μ_v, which is related to the parallel current-density, $\mu = \mathbf{j}\cdot\mathbf{B}/B^2$. In this case the helicity will only be known *a posteori*.

It is sometimes desirable to allow the value of $K_{v,0}$ and μ_v, and either one or both of $\Delta\psi_{t,v}$ and $\Delta\psi_{p,v}$ to vary in order to obtain solutions with, for example, prescribed rotational transform on the interfaces, or to constrain the currents passing through certain surfaces. This will be discussed below.

C. free-boundary

The MRxMHD energy functional just described can easily be generalized to describe free-boundary equilibria by including an additional volume that lies outside the plasma in which the vacuum field is to be calculated. Vacuum fields satisfy $\nabla\times\mathbf{B} = 0$, and so are of course a special class of Beltrami fields, namely Beltrami fields with $\mu = 0$. Most of the existing numerical architecture developed for fixed-boundary SPEC [12] can be employed for free-boundary SPEC .

The inner boundary of this additional region is coincident with the plasma boundary. The outer boundary, hereafter called the "computational boundary", is arbitrary except that the computational boundary must lie between the plasma boundary and the external current-carrying coils. (Including a filamentary representation of the external coils, for example, would result in singularities in the magnetic field if they were to be included in the computational domain.) The computational boundary may be taken as a smooth approximation to the vacuum vessel, for example.

The normal magnetic field on the computational boundary is not required to be zero and magnetic field-lines can enter and leave the computational boundary. The enclosed toroidal and poloidal fluxes, $\Delta\psi_t$ and $\Delta\psi_p$, in the vacuum region are not well-defined *physical* quantities. As will be described in the following, $\Delta\psi_t$ and $\Delta\psi_p$ in the vacuum region can be iteratively adjusted to enforce constraints on the total toroidal plasma current, I, and the external coil current, G, linking the torus.

Given the geometry of the computational boundary, $\mathbf{x}(\theta,\phi)$, where θ and ϕ are poloidal and toroidal angles, the normal field magnetic field at the computational boundary is, for convenience, written as $\mathbf{B}\cdot\mathbf{x}_\theta\times\mathbf{x}_\phi = B^n$, where $\mathbf{x}_\theta \equiv \partial\mathbf{x}/\partial\theta$ and $\mathbf{x}_\phi \equiv \partial\mathbf{x}/\partial\phi$. This has two components, $B^n \equiv B^n_P + B^n_C$, a part produced by plasma currents, B^n_P, which is *a priori* unknown and must be computed self-consistently as part of the equilibrium calculation; and a part produced by "coil" currents external to the computational domain, B^n_C, and this part is required as input.

The geometry of the ideal interfaces, $\mathcal{I}_v$ for $v = 1,\ldots,N_V$, which includes the plasma boundary,

is adjusted iteratively to construct a free-boundary equilibrium that is consistent with force balance, $[[p + B^2/2]] = 0$ across each of the $\mathcal{I}_v$. The computational boundary and B_C^n need not change during the calculation. (Whether there is some computational advantage in allowing the computational boundary to change during the free-boundary iterations will be decided by future work.)

D. numerical implementation

All even, doubly periodic functions are expressed using the following abbreviated representation for a double Fourier series,

$$\begin{aligned}&\sum_i f_i \cos(m_i\theta - n_i\phi)\\ \equiv\ &\sum_{n=0}^{N} f_{0,n}\cos(-n\phi)\\ +\ &\sum_{m=1}^{M}\sum_{n=-N}^{N} f_{m,n}\cos(m\theta - nN_P\phi),\end{aligned} \tag{5}$$

where M and N are the Fourier resolutions, and N_P is the field periodicity; and similarly for the odd functions. This representation avoids redundancies.

The equilibrium calculation is initialized by providing a reasonable initial guess for the geometry of the $v = 1, \ldots, N_V$ ideal interfaces, $\mathbf{x}_v(\theta,\phi) \equiv R_v(\theta,\phi)\cos\phi\ \hat{i} + R_v(\theta,\phi)\sin\phi\ \hat{j} + Z_v(\theta,\phi)\ \hat{k}$, where $R_v \equiv \sum_i \left[R^c_{i,v}\cos(m_i\theta - n_i\phi) + R^s_{i,v}\sin(m_i\theta - n_i\phi)\right]$, and similarly for Z_v, and by providing a similar representation for the computational boundary. The poloidal angle parameterization, θ, is at this stage arbitrary. The toroidal angle, ϕ, used hereafter is the standard geometric cylindrical angle.

SPEC can operate in Cartesian [14] (i.e., slab), cylindrical [16, 17] and toroidal [12] geometry; but, for brevity, the following will restrict attention to the toroidal case. SPEC also allows for arbitrary, non-stellarator-symmetric geometry; again, for brevity, the following shall display only the stellarator-symmetric terms.

Given the geometry of the ideal interfaces and the computational boundary, $\mathbf{x}_v(\theta,\phi)$ for $v = 1, \ldots, N_V + 1$, a continuous toroidal coordinate framework can be defined by interpolation. In the *annular* volumes, $\mathcal{V}_v$ for $v = 2, \ldots, N_V + 1$, which are bounded by $\mathbf{x}_{v-1}(\theta,\phi)$ and $\mathbf{x}_v(\theta,\phi)$, the coordinates are defined by $\mathbf{x}(s,\theta,\phi) \equiv \frac{1}{2}(1-s)\ \mathbf{x}_{v-1}(\theta,\phi) + \frac{1}{2}(1+s)\ \mathbf{x}_v(\theta,\phi)$, where the "local" radial coordinate varies from $s = -1$ at the inner boundary to $s = +1$ at the outer boundary. (A global radial coordinate is not required; the calculation of the magnetic field in each region is computed in parallel.) The coordinate interpolation is implemented in Fourier space, $R^c_i(s) = \frac{1}{2}(1-s)R^c_{i,v-1} + \frac{1}{2}(1+s)R^c_{i,v}$, and similarly for the Z^s_i.

In the innermost *simple-torus* volume, $\mathcal{V}_1$, which is bounded by $\mathcal{I}_1 \equiv \mathbf{x}_1(\theta,\phi)$, the coordinates are constructed by first defining the "geometric center" of $\mathcal{I}_1$,

$$R_0(\phi) \equiv \frac{\oint R_1(\theta,\phi)\ dl}{L(\phi)}, \tag{6}$$

$$Z_0(\phi) \equiv \frac{\oint Z_1(\theta,\phi)\ dl}{L(\phi)}, \tag{7}$$

to be the coordinate axis, where the poloidal arclength is $L(\phi) \equiv \oint dl$, and $dl/d\theta \equiv \sqrt{\partial_\theta R_1(\theta,\phi)^2 + \partial_\theta Z_1(\theta,\phi)^2}$. The coordinate axis serves as the degenerate, $v = 0$ interface. Introducing $\bar{s} \equiv (s+1)/2$, so that $\bar{s} \in [0,1]$, the coordinates in the innermost volume are defined by the following "regularized" interpolation

$$R^c_i(s) = R^c_{i,0} + (R^c_{i,1} - R^c_{i,0})f_i, \tag{8}$$

where $f_i = \bar{s}$ for $m_i = 0$, and $f_i = \bar{s}^{m_i/2}$ for $m \neq 0$, and similarly for the Z^s_i. Such a construction encourages, but provides no guarantee, that the coordinate surfaces will not intersect. (For strongly shaped configurations, this coordinate interpolation may need to be revised.) This interpolation implies that the approximate minor radius of each coordinate surface scales like $r \sim \sqrt{s}$.

In each volume, a mixed Fourier-Chebyshev representation is used for the vector potential, $\mathbf{A}$. An appropriate gauge [12] allows $\mathbf{A} = A_\theta\nabla\theta + A_\phi\nabla\phi$. The components of the vector potential are written

$$A_\theta(s,\theta,\phi) = \sum_i \sum_{l=0}^{L} A_{\theta,e,i,l}\ T_l(s)\cos(m_i\theta - n_i\phi), \tag{9}$$

where L describes the Chebyshev resolution in a given region, and similarly for $A_\phi(s,\theta,\phi)$. Additional odd (i.e., sine) harmonics are also included for the non-stellarator-symmetric case. The Chebyshev polynomials, $T_l(s)$, are determined using recurrence relations: $T_0(s) = 1$, $T_1(s) = s$, and $T_l(s) = 2\,s\,T_{l-1}(s) - T_{l-2}(s)$ thereafter.

To accommodate the coordinate singularity that arises at the coordinate axis, in the innermost toroidal region this representation is augmented with "radial regularization factors", so that $T_l(s)\cos(m_i\theta - n_i\phi) \rightarrow \bar{s}^{m_i/2}T_l(s)\cos(m_i\theta - n_i\phi)$, for example.

Coordinate surfaces coincide with the $\mathcal{I}_v$ and the computational boundary, and this by design makes it easy to enforce the constraints on the magnetic vector potential so that $\mathbf{B}\cdot\mathbf{x}_\theta\times\mathbf{x}_\phi = 0$ on the $\mathcal{I}_v$ and $\mathbf{B}\cdot\mathbf{x}_\theta\times\mathbf{x}_\phi = B^n$ on the computational boundary; but elsewhere in the relaxed volumes there is no assumed relationship between the coordinates and the structure of the magnetic field, which at this stage is yet to be determined.

The boundary condition that $\mathbf{B}\cdot\mathbf{x}_\theta\times\mathbf{x}_\phi = 0$ at the inner boundary of each region is enforced, and the remaining gauge freedom constrained, by requiring that $A_\theta(-1,\theta,\phi) = 0$ and $A_\phi(-1,\theta,\phi) = 0$. The condition that $\mathbf{B}\cdot\mathbf{x}_\theta\times\mathbf{x}_\phi = B^n$ at the outer boundary requires that $\partial_\theta A_\phi(+1,\theta,\phi) - \partial_\phi A_\theta(+1,\theta,\phi) = B^n$. This condition, and the constraints on the enclosed toroidal and poloidal fluxes, $\Delta\psi_{t,v}$ and $\Delta\psi_{p,v}$, and the helicities, $K_{v,0}$, in each region are enforced using Lagrange multipliers.

Temporarily ignoring the pressure, which does not alter the solution of the Beltrami fields in each $\mathcal{V}_v$ and only impacts the constraint of force balance, $[[p + B^2/2]] = 0$

across the ideal interfaces, the degrees-of-freedom in the constrained energy functional in each volume are the coefficients of the Fourier-Chebyshev representation for the vector potential and the various Lagrange multipliers. Writing $\mathbf{a} \equiv \{A_{\theta,e,i,l}, A_{\phi,e,i,l}, \mu, a_i, b_i, c_1, d_1, e_i\}$, and dropping the "$v$" subscript for clarity, in each volume we have

$$\begin{aligned}\mathcal{F}[\mathbf{a}] \equiv & \frac{1}{2}\int_{\mathcal{V}} \mathbf{B}\cdot\mathbf{B}\; dv - \frac{\mu}{2}\left[\int_{\mathcal{V}} \mathbf{A}\cdot\mathbf{B}\; dv - K_0\right] \\ & + a_i \left[\sum_l A_{\theta,e,i,l} T_l(-1)\right] \\ & + b_i \left[\sum_l A_{\phi,e,i,l} T_l(-1)\right] \\ & + c_1 \left[\sum_l A_{\theta,e,1,l} T_l(+1) - \Delta\psi_t\right] \\ & + d_1 \left[\sum_l A_{\phi,e,1,l} T_l(+1) - \Delta\psi_p\right] \\ & + e_i \left[\sum_l \left(-m_i A_{\phi,e,i,l} - n_i A_{\theta,e,i,l}\right) T_l(+1) - B^n_{o,i}\right]\end{aligned} \tag{10}$$

where the a_i and b_i are Lagrange multipliers used to enforce the combined gauge and boundary conditions on the inner boundary, c_1 and d_1 are Lagrange multipliers used to enforce the enclosed flux constraints, and the e_i are Lagrange multipliers used to enforce the boundary condition $\mathbf{B}\cdot\mathbf{x}_\theta \times \mathbf{x}_\phi = B^n$ on the outer boundary; and summation over i is assumed.

In each of the plasma volumes the outer boundary condition is $B^n_{o,i} = 0$, and $B^n \neq 0$ is only allowed at the computational boundary. In the innermost volume there is no constraint on the enclosed poloidal flux and we may set $d_1 = 0$.

The energy functional can be written

$$\mathcal{F} = \tfrac{1}{2}\mathbf{a}^T\mathcal{A}\,\mathbf{a} + \tfrac{1}{2}\mu\,\mathbf{a}^T\mathcal{B}\,\mathbf{a} + \mathbf{a}^T\mathcal{C}\,\mathbf{b}, \tag{11}$$

where $\mathcal{A}$, $\mathcal{B}$ and $\mathcal{C}$ are matrices that depend only on the geometry of the adjacent interfaces; and $\mathbf{b}$ represents the boundary conditions, namely $(\Delta\psi_t, \Delta\psi_p, K_o)^T$ and the "odd" Fourier harmonics of the total normal field on the outer interface, $B^n_{o,i}$. (For non-stellarator-symmetric calculations, the normal field on the computational boundary will also include cosine harmonics.)

As described above, the total normal magnetic field, $B^n = B^n_P + B^n_C$, at the computational boundary is not yet known. It depends in part on the plasma currents. That part of the normal magnetic field that is produced by the coil currents, B^n_C, is known *a priori* and is required as input. To initialize the free-boundary calculation, a reasonable initial guess, e.g., $B^n_P = -B^n_C$, is required. This will be re-evaluated as the free-boundary iterations proceed, as described below, to obtain a self-consistent solution.

The extremizing states are determined by solving $\nabla_{\mathbf{a}}\mathcal{F} = 0$.

The constrained energy functional, $\mathcal{F}$, is close to being quadratic in the degrees-of-freedom; except for the $\frac{1}{2}\mu\,\mathbf{a}^T\mathcal{B}\,\mathbf{a}$ term, it is quadratic. If $\mathcal{F}$ *were* strictly quadratic in $\mathbf{a}$, then $\nabla_{\mathbf{a}}\mathcal{F} = 0$ would reduce to a set of linear equations, the coefficients of which would be given by the second derivatives of $\mathcal{F}$; and this would allow some reduction in the computational burden. This is also true if μ were to be treated as parameter, rather than as a degree-of-freedom: the equation $\nabla\times\mathbf{B} = \mu\mathbf{B}$ is, given μ, a linear equation for $\mathbf{B}$, namely $(\mathcal{A}+\mu\mathcal{B})\,\mathbf{a}+\mathcal{C} = 0$. Non-trivial solutions are obtained by providing non-trivial enclosed toroidal and poloidal fluxes.

Generally, however, to be consistent with the method of Lagrange multipliers, μ must be treated as an independent degree-of-freedom that is to be adjusted in order to enforce the helicity constraint, and a Newton method must be used to find extrema. Once the $\mathcal{A}$, $\mathcal{B}$ and $\mathcal{C}$ as defined by Eqn. 11 are computed, the Newton iterations are quite rapid.

The $\int \mathbf{A}\cdot\mathbf{B}\; dv \equiv \mathbf{a}^T\mathcal{B}\,\mathbf{a}$ integral has a simple form. The Jacobian factors cancel and no coordinate metric information is required. The most-complicated non-zero second derivatives of this term are given by

$$\begin{aligned}&\frac{\partial}{\partial A_{\phi,e,j,p}}\frac{\partial}{\partial A_{\theta,e,i,l}}\int \mathbf{A}\cdot\mathbf{B}\; dv \\ &= \iiint T_{p,j}\cos\alpha_j T'_{l,i}\cos\alpha_i\; ds\, d\theta\, d\phi \\ &- \iiint T_{l,i}\cos\alpha_i T'_{p,j}\cos\alpha_j\; ds\, d\theta\, d\phi,\end{aligned} \tag{12}$$

which are not particularly complicated at all. These are independent of geometry, and so only need to be computed once, and they can be computed analytically.

The second derivatives of the $\int \mathbf{B}\cdot\mathbf{B}\; dv \equiv \mathbf{a}^T\mathcal{A}\,\mathbf{a}$ integral with respect to the $A_{\theta,e,i,l}$ and $A_{\phi,e,i,l}$ amount to volume integrals of the products of the Chebyshev polynomials and their derivatives, trigonometric terms, and the coordinate metrics and Jacobian; and thus they depend on the geometry of the adjacent interfaces and need to be re-evaluated each time the interface geometry is changed.

The required volume integrals are computed using a mixed "Fourier-Gaussian" quadrature method:

$$\begin{aligned}&\int_{-1}^{+1}\int_0^{2\pi}\int_0^{\frac{2\pi}{N_P}} f(s,\theta,\phi)\;\; d\phi\, d\theta\, ds \\ &\approx \frac{2\pi}{N_P} 2\pi \sum_{k=1}^{K} \omega_k\, f_1^c(s_k),\end{aligned} \tag{13}$$

where first a Fast Fourier Transform (FFT) allows $f = \sum_i \left[f_i^c\cos(m_i\theta - n_i\phi) + f_i^s\sin(m_i\theta - n_i\phi)\right]$, and where the ω_k and s_k are the weights and abscissae for a Gaussian integration of resolution K. (A good check on the numerics is to compute the integrals in Eqn. 12 using the Fourier-Gaussian quadrature and compare to the analytic expressions.)

Given that the magnetic fields in each region have been calculated – either by a single linear solve or by an iterative Newton method – it is then possible to determine the rotational-transform on the ideal interfaces and the enclosed plasma currents. Depending on the particular class of equilibrium solution that one seeks, these may play an important role in the calculation.

On flux surfaces, a straight fieldline angle, θ_s, may be constructed with a transformation, $\theta_s = \theta + \sum_i \lambda_i \sin(m_i\theta - n_i\phi)$, by insisting that

$$\frac{\mathbf{B}\cdot\nabla\theta_s}{\mathbf{B}\cdot\nabla\phi} = \dot{\theta}(1+\lambda_\theta) + \lambda_\phi = \iota, \tag{14}$$

where $\boldsymbol{\lambda} \equiv (\iota, \lambda_1, \lambda_2, \ldots)^T$ is to be determined. Writing $\dot{\theta} = -\partial_s A_\phi / \partial_s A_\theta$, this becomes

$$\partial_s A_\theta\, \iota + \partial_s A_\phi\, \lambda_\theta - \partial_s A_\theta\, \lambda_\phi = -\partial_s A_\phi. \tag{15}$$

(For non-stellarator-symmetry additional cosine terms will need to be included in the angle transformation.) If $\mathbf{A}$ is given, equating the Fourier coefficients of each side amounts to a set of linear equations for $\boldsymbol{\lambda}$.

There is a quirk associated with rational rotational-transform surfaces: the transformation to the straight fieldline angle is not unique; however, the rotational transform is still well-defined. So, even on rational surfaces, the set of linear equations defined by Eqn. 15 can be solved using Singular Value Decomposition (SVD).

In MRxMHD, only the ideal interfaces are guaranteed by constraint to remain as intact flux surfaces during the calculation. Given that sheet currents on the ideal interfaces are both mathematically admittable and physically meaningful in the context of ideal MHD [16], the transformation to the straight fieldline angle may be multi-valued on the ideal interfaces. The rotational-transform on the "inner" side of $\mathcal{I}_v$ is determined by the tangential field in $\mathcal{V}_v$, and that on the "outer" side is determined by the tangential field in $\mathcal{V}_{v+1}$.

For an *a priori* specification of $(\Delta\psi_{t,v}, \Delta\psi_{p,v}, K_{v,0})^T$ in each subregion, or $(\Delta\psi_{t,v}, \Delta\psi_{p,v}, \mu_v)^T$ if the helicity-multiplier is to be constrained rather than the helicity itself, the rotational-transform on the interfaces can only be determined *a posteori*. The calculation of the Beltrami field in any region is independent of the calculation in any other region, and there is no reason to generally expect that the rotational-transform is continuous across the ideal interfaces.

To enforce the rotational-transform on each $\mathcal{I}_v$ to be a prescribed value, and keeping the constraint of conserved enclosed toroidal flux in each region, it is generally required to iterate on $\Delta\psi_{p,v}$, and either $K_{o,v}$ or μ_v, to match the required values of the rotational-transform on the inner and outer boundaries of each region. A similar argument holds for the enclosed currents.

The total current passing through a given surface is determined by a surface integral of the current-density, equivalently a line integral of the magnetic field,

$$\int_{\mathcal{S}} \mathbf{j}\cdot d\mathbf{s} = \int_{\partial\mathcal{S}} \mathbf{B}\cdot d\mathbf{l}\,. \tag{16}$$

The total toroidal plasma current, including any sheet currents that may lie on the plasma boundary, is obtained by taking a "poloidal loop", $d\mathbf{l} \equiv \mathbf{e}_\theta\, d\theta$, lying on the inner surface of the vacuum region (i.e., on the immediate outside of the plasma boundary), to obtain

$$I = \int_0^{2\pi} \left(-\partial_s A_\phi\; g_{\theta\theta} + \partial_s A_\theta\; g_{\theta\phi}\right)/\sqrt{g}\, d\theta. \tag{17}$$

The "linking" current through the torus is obtained by taking a "toroidal loop", $d\mathbf{l} \equiv \mathbf{e}_\phi\, d\phi$, to obtain

$$G = \int_0^{2\pi} \left(-\partial_s A_\phi\; g_{\theta\phi} + \partial_s A_\theta\; g_{\phi\phi}\right)/\sqrt{g}\, d\phi. \tag{18}$$

To match the required values for I and G, the values of $(\Delta\psi_{t,v}, \Delta\psi_{p,v})^T$ in the vacuum region must be adjusted accordingly, with $\mu_v = 0$.

Given the geometry of the ideal interfaces and having solved the Beltrami fields in each volume, it is then required to iteratively adjust the geometry of the $\mathcal{I}_v$ to satisfy force balance across the interfaces, namely that $[[p + B^2/2]] = 0$. For this it is possible to use a conjugate-gradient method (assuming that the helicity constraint is enforced in each region). This approach has the advantages of robustly locating a *minimum* energy state, rather than an *extremum* of $\mathcal{F}$. If, instead, the helicities in each region are to be adjusted in order to satisfy a rotational-transform constraint, a multi-dimensional Newton method can be used to iteratively determine the geometry of the $\mathcal{I}_v$.

To constrain the tangential degrees-of-freedom, additional "spectral constraints" are included [12, 24, 25].

There is one last step that is required to obtain a free-boundary equilibrium that is consistent with the supplied external magnetic field: namely, to determine the self-consistent normal magnetic field at the computational boundary that is produced by the plasma currents, B^n_P.

Given the tangential field on the plasma boundary,

$$\mathbf{B}_s = B^\theta \mathbf{e}_\theta + B^\phi \mathbf{e}_\phi, \tag{19}$$

the virtual casing principle [26–28] shows that the magnetic field outside the plasma produced by internal plasma currents is equivalent to the field generated by the surface current $\mathbf{j} = \mathbf{B}_s \times \mathbf{n}$, where $\mathbf{n}$ is normal to the surface. The field created by this surface current is given by

$$\mathbf{B}(\bar{\mathbf{x}}) = \int_{\mathcal{S}} \frac{(\mathbf{B}_s \times d\mathbf{s})\times\hat{\mathbf{r}}}{r^2}, \tag{20}$$

where $d\mathbf{s} \equiv \mathbf{e}_\theta \times \mathbf{e}_\phi\, d\theta d\phi$.

After the iterations have converged to a solution that globally satisfies force balance for a given $B^n_P + B^n_C$, the value of B^n_P consistent with the constructed equilibrium can be efficiently determined using Eqn. 20.

Generally, the normal field thus computed will not be the same as the normal field as initially supplied to Eqn. 10. Picard iterations provide a practical solution to this problem: the normal field used for the next "free-boundary" iteration is given by

$$B^n_P \to \lambda B^n_P + (1-\lambda) B^n_{vc}, \tag{21}$$

where B^n_{vc} is the normal field as computed using Eqn. 20, and $0 \le \lambda \le 1$ is a blending parameter used to provide numerical stability. These iterations are deemed to have converged when $|B^n_{vc} - B^n_P|$ is less than a user-provided tolerance.

A specific *fixed*-boundary SPEC equilibrium is described by the plasma boundary, and the given pressure, the enclosed toroidal and poloidal fluxes, and the

helicity in each subregion, $(p_v, \Delta\psi_{t,v}, \Delta\psi_{p,v}, K_v)$. Iterations over the helicity multipler μ_v are generally required to determine the value consistent with the helicity constraint. Alternatively, the helicity multiplier itself may be given directly, so that an equilibrium may be described by $(p_v, \Delta\psi_{t,v}, \Delta\psi_{p,v}, \mu_v)$. It is also possible to define the equilibrium by providing the rotational-transform on the inner and outer interfaces in each subregion, $(p_v, \Delta\psi_{t,v}, \iota_v^-, \iota_v^+)$, and this will generally require an iteration over both $\Delta\psi_{p,v}$ and μ_v. The total toroidal flux enclosed by the plasma boundary, Φ, is also required.

For a *free*-boundary SPEC calculation, it is required to also provide: (i) a computational boundary that lies inside the external coils and outside the expected location of the plasma boundary, where the self-consistent plasma boundary will be determined iteratively; (ii) the magnetic field normal to the computational boundary, $B_C^n \equiv \mathbf{B}_C \cdot \mathbf{x}_\theta \times \mathbf{x}_\phi$, produced by the external set of current coils; and (iii) the total enclosed "plasma" and "linking" currents, I and G.

E. illustration in stellarator geometry

Non-axisymmetric configurations can produce rotational-transform with no plasma currents [29]. We can thus verify SPEC vacuum solutions against a Biot-Savart code by constructing a suitable "stellarator" vacuum field.

The newly developed FOCUS code [30] is used to construct a set of filamentary current-carrying coils that produce a magnetic field suitable for SPEC verification calculations. Given a desired "plasma boundary", and a finite number of modular coils that are represented as closed, one-dimensional loops embedded in three-dimensional space each carrying a current I_i, FOCUS adjusts the geometry of the coils, subject to engineering constraints, and the coil currents to minimize $\frac{1}{2}\int(\mathbf{B}_C \cdot \mathbf{n})^2 ds$ on the plasma boundary, where $\mathbf{n}$ is normal and $\mathbf{B}_C$ is the "coil" field as computed using Biot-Savart. To avoid trivial solutions, an additional constraint on the total enclosed toroidal flux is also included, e.g. $\Phi = 1$.

The non-stellarator-symmetric, non-axisymmetric "target" plasma boundary considered here is

$$\begin{aligned} R(\theta,\phi) &= R_a(\theta) + \delta R(\theta,\phi), \\ Z(\theta,\phi) &= Z_a(\theta) + \delta Z(\theta,\phi), \end{aligned} \tag{22}$$

where $R_a(\theta) = 3 + 0.3\cos\theta$ and $Z_a(\theta) = -0.3\sin\theta$, and $\delta R(\theta,\phi) = -0.06\cos(\theta - N_P\,\phi) + 0.03\sin(\theta - N_P\,\phi) + 0.03\sin(-N_P\,\phi)$ and $\delta Z(\theta,\phi) = -0.06\sin(\theta - N_P\,\phi) - 0.06\sin(-N_P\,\phi)$; and where the field periodicity is $N_P = 2$. This surface is shown on three different cross section in Fig. 1. FOCUS rapidly determines a coil arrangement that provides an excellent approximation to the given boundary.

Note: the following SPEC verification calculation does not depend on how precisely the above surface is recovered as a flux surface of the external vacuum field. Hereafter, the coil arrangement is assumed to be completely arbitrary. All that is required is B_C^n, the magnetic field normal to the computational boundary produced by the external current-carrying coils, and the coil linking current, G.

The computational boundary considered here is the same as that given in Eqn. 22 but slightly larger, $R_a(\theta) = 3 + 0.45\cos\theta$ and $Z_a(\theta) = -0.45\sin\theta$. Both the odd and even Fourier harmonics of the normal magnetic field, B_C^n, produced by the external currents are easily computed using Biot-Savart. For vacuum calculations, the required total plasma current, I, is zero. The linking current, G, is directly obtained from the coil configuration.

For vacuum calculations, for which there are no plasma currents, an excellent *a priori* guess for B_P^n is available, namely $B_P^n = 0$. It is required to constrain the helicity multipliers in each region appropriately, namely $\mu_v = 0$. The Beltrami fields in each region are then parameterized by the enclosed toroidal and poloidal fluxes in each region, $(\Delta\psi_{t,v}, \Delta\psi_{p,v})^T$.

However; to recover the vacuum solution it is *not* sufficient merely to constrain the $\mu_v = 0$. Doing so does ensure that there are no *volume* currents in the plasma domains, but this does not ensure that there are no *sheet* currents on the $\mathcal{I}_v$. Sheet currents inside the plasma domain means that the solution is not a vacuum, and such currents may result in discontinuities in the rotational-transform across the $\mathcal{I}_v$.

The toroidal current, δI_v passing through an infinitesimally thin cross-sectional surface on for example the $\phi = 0$ plane with inner boundary just inside a given $\mathcal{I}_v$ and outer boundary just outside is given by

$$\delta I_v \equiv \int_0^{2\pi} \left(\mathbf{B}^+ - \mathbf{B}^-\right) \cdot \mathbf{e}_\theta \; d\theta, \tag{23}$$

where $\mathbf{B}^+$ is the tangential field immediately outside $\mathcal{I}_v$ in region $\mathcal{V}_{v+1}$ and $\mathbf{B}^-$ is the tangential field immediately inside $\mathcal{I}_v$ in region $\mathcal{V}_v$. To fully constrain the calculation to recover the vacuum solution, additional constraints are required, namely that the δI_v are zero. This can easily be enforced by allowing the $\Delta\psi_{p,v}$ to vary.

For this vacuum calculation, because there are no internal plasma currents, the virtual casing calculation of B_P^n is not required.

A comparison of the Poincaré plots produced with the magnetic field calculated with an $N_V = 2$ free-boundary SPEC calculation and that calculated directly from the Biot-Savart law given the coil geometries and currents is shown in Fig. 1.

Recall that N_V indicates the number of regions in the plasma domain, so that for free-boundary calculations there are $N_V + 1$ regions in the multi-region decomposition. Choosing $N_v = 2$ is the minimum that simultaneously tests the numerical calculation in the simple-torus region with $v = 1$, the toroidal annular regions with $v = 2, \ldots, N_V$, and the vacuum region with $v = N_V + 1$. Adding additional regions to the calculation merely adds additional toroidal annular regions.

Fig. 2 shows the error,

$$\Delta \equiv \int_{\mathcal{V}} |\mathbf{B}_S - \mathbf{B}_C| \; dv, \tag{24}$$

defined as an integral over the plasma volume of the difference between the computed SPEC magnetic field, B_S,

and the field calculated directly using the Biot-Savart formula with the given coil geometries and currents, B_C, plotted against Fourier resolution. This error reliably decreases as the numerical resolution is increased. The radial (Chebyshev) resolution is $L = 8$ in each region.

F. illustration in tokamak geometry

For the above stellarator-geometry, vacuum verification calculation it was not required to exercise the virtual casing calculation. The vacuum solution was sought, so it was appropriate and expedient to assume $B^n_P = 0$. Generally, and most obviously for axisymmetric equilibria, it is required to include the magnetic field produced by the plasma.

The second verification calculation we present is for an axisymmetric configuration. The computational boundary is a circular cross-section axisymmetric toroidal surface of major radius $R_0 = 1.00m$ and minor radius $r = 0.45m$, on which the $(m, n) = (1, 0)$ and $(2, 0)$ sine and cosine harmonics of B^n_C are manually adjusted to create a single-null tokamak, as is shown in Fig. 3. Note that the separatrix is allowed in the vacuum region.

The initial geometry of the ideal interfaces is that of nested, circular cross section, axisymmetric tori. The initial guess for the normal field on the computational boundary produced by the plasma currents is $B^n_P = -B^n_C$, and the Picard blend parameter on B^n_P appearing in Eqn. 21 is $\lambda = 0.4$.

The pressure profile is a stepped approximation to $p(\psi) = 1 - 2\psi + \psi^2$ where ψ is the normalized toroidal flux. The rotational transform constraints in each subregion are enforced by iterating on the enclosed poloidal fluxs and helicity multipliers.

For this calculation, we choose $N_V = 7$, the poloidal and toroidal Fourier resolutions are $M = 6$ and $N = 0$, and the Chebyshev resolution in each region is $L = 6$.

G. scaling

The equilibria are invariant under the following transformation: $\Phi \to \lambda\Phi$, $I \to \lambda I$, $G \to \lambda G$, $p \to \lambda^2 p$, $B^n_C \to \lambda B^n_C$, The internal numerics normalizes $\Delta\psi_{t,v}$ and $\Delta\psi_{p,v}$ to Φ. The helicity multipliers and the rotational-transforms in each region do not change.

H. future work

The initial priority regarding development of SPEC was to confirm accuracy and reliability. Verification calculations thus far published have included: But, there is a great deal of computational efficiencies that are yet to be exploited. Future numerical work on developing the SPEC code will concentrate on exploiting various symmetries in the matrix constructions and so forth for speed.

An immediate physics application for free-boundary SPEC is to explicitly calculate the effect of resonant magnetic perturbations on the unstable manifold surrounding the plasma.

This manuscript is based upon work supported by the U.S. Department of Energy, Office of Science, Office of Fusion Energy Sciences, and has been authored by Princeton University under Contract Number DE-AC02-09CH11466 with the U.S. Department of Energy.

[1] M. J. Hole, S. R. Hudson, and R. L. Dewar. Stepped pressure profile equilibria in cylindrical plasmas via partial Taylor relaxation. *J. Plasma Phys.*, 72(6):1167, 2006.

[2] M. J. Hole, S. R. Hudson, and R. L. Dewar. Equilibria and stability in partially relaxed plasma-vacuum systems. *Nucl. Fus.*, 47:746, 2007.

[3] S. R. Hudson, M. J. Hole, and R. L. Dewar. Eigenvalue problems for Beltrami fields arising in a three-dimensional toroidal magnetohydrodynamic equilibrium problem. *Phys. Plasmas*, 14:052505, 2007.

[4] O. P. Bruno and P. Laurence. Existence of three-dimensional toroidal MHD equilibria with nonconstant pressure. *Commun. Pur. Appl. Math.*, 49(7):717, 1996.

[5] J. Moser. *Stable and Random Motions.* Princeton Univ. Press,, Princeton, N. J., 1973.

[6] V. I. Arnold. *Mathematical methods of Classical Mechanics.* Springer-Verlag Press, New York, 1978.

[7] G. R. Dennis, S. R. Hudson, R. L. Dewar, and M. J. Hole. Multi-region relaxed magnetohydrodynamics with flow. *Phys. Plasmas*, 21(4):042501, 2014.

[8] G. R. Dennis, S. R. Hudson, R. L. Dewar, and M. J. Hole. Multi-region relaxed magnetohydrodynamics with anisotrophy and flow. *Phys. Plasmas*, 21(7):072512, 2014.

[9] M. Lingam, H. M. Abdelhamid, and S. R. Hudson. Multi-region relaxed Hall magnetohydrodynamics with flow. *Phys. Plasmas*, 23(8):082103, 2016.

[10] R.L. Dewar, Z. Yoshida, A. Bhattacharjee, and S.R. Hudson. Variational formulation of relaxed and multi-region relaxed magnetohydrodynamics. *J. Plasma Phys.*, 81:515810604, 2015.

[11] S. R. Hudson and B. Kraus. Smooth magnetohydrodynamic equilibria with arbitrary, three-dimensional boundaries. *draft*, 2017.

[12] S. R. Hudson, R. L. Dewar, G Dennis, M. J. Hole, M. McGann, G. von Nessi, and S. Lazerson. Computation of multi-region relaxed magnetohydrodynamic equilibria. *Phys. Plasmas*, 19:112502, 2012.

[13] G. R. Dennis, S. R. Hudson, D. Terranova, P. Franz, R. L. Dewar, and M. J. Hole. Minimally constrained model of self-organized helical states in reversed-field pinches. *Phys. Rev. Lett.*, 111:055003, 2013.

[14] J. Loizu, S. R. Hudson, A. Bhattacharjee, and P. Helander. Magnetic islands and singular currents at rational surfaces in three-dimensional MHD equilibria. *Phys. Plasmas*, 22:022501, 2015.

[15] G. R. Dennis, S. R. Hudson, R. L. Dewar, and M. J. Hole. The infinite interface limit of multiple-region relaxed magnetohydrodynamics. *Phys. Plasmas*, 20:032509, 2013.

[16] J. Loizu, S. R. Hudson, A. Bhattacharjee, S. Lazerson,

and P. Helander. Existence of three-dimensional ideal-MHD equilibria with current sheets. *Phys. Plasmas*, 22:090704, 2015.
[17] J. Loizu, S. R. Hudson, Helander, Lazerson, and Bhattacharjee. Pressure-driven amplification and penetration of resonant magnetic perturbations. *Phys. Plasmas*, 23(5):055703, 2016.
[18] J. Loizu, S. R. Hudson, and C. Nührenberg. Verification of the SPEC code in stellarator geometries. *Phys. Plasmas*, 23(11):112505, 2016.
[19] M. D. Kruskal and R. M. Kulsrud. Equilibrium of a magnetically confined plasma in a toroid. *Phys. Fluids*, 1(4):265, 1958.
[20] J. B Taylor. Relaxation of toroidal plasma and generation of reverse magnetic-fields. *Phys. Rev. Lett.*, 33:1139, 1974.
[21] J. M. Finn and T. M. Antonsen Jr. Magnetic helicity: What is it and what is it good for? *Comments Plasma Phys. Control. Fusion*, 9:111, 1985.
[22] J. B Taylor. Relaxation and magnetic reconnection in plasmas. *Rev. Mod. Phys.*, 58:741, 1986.
[23] M. McGann, S. R. Hudson, R. L. Dewar, and G. von Nessi. Hamilton-jacobi theory for continuation of magnetic field across a toroidal surface supporting a plasma pressure discontinuity. *Phys. Lett. A*, 374(33):3308, 2010.
[24] S. P. Hirshman and H. K. Meier. Optimized fourier representations for three-dimensional magnetic surfaces. *Phys. Fluids*, 28(5):1387, 1985.
[25] S. P. Hirshman and J. Breslau. Explicit spectrally optimized fourier series for nested magnetic surfaces. *Phys. Plasmas*, 5(7):2664, 1998.
[26] V. D. Shafranov and L. E. Zakharov. Use of the virtual-casing principle in calculating the containing magnetic field in toroidal plasma systems. *Nucl. Fus.*, 12:599, 1972.
[27] S.A. Lazerson. The virtual-casing principle for 3D toroidal systems. *Plasma Phys. Contr. F*, 54:122002, 2012.
[28] J. D. Hanson. The virtual-casing principle and Helmholtz's theorem. *Plasma Phys. Contr. F*, 57:115006, 2015.
[29] P. Helander. Theory of plasma confinement in non-axisymmetric magnetic fields. *Rep. Prog. Phys.*, 77(8):087001, 2014.
[30] C. Zhu and S. R. Hudson. Focus: Flexible optimized coils using space curves. *draft*, 2017.

1. Appendix: Why not use the scalar potential?

The algorithm in SPEC used to compute the vacuum magnetic field represented the magnetic field as the curl of the magnetic vector potential. This would seem somewhat inefficient, as vacuum fields can be represented by a scalar potential, $\mathbf{B} = \nabla\Phi$, where

$$\Phi = I\theta + G\phi + \tilde{\Phi}(s,\theta,\phi), \tag{25}$$

where I and G and the plasma and linking currents and $\tilde{\Phi}(s,\theta,\phi)$ is a single-valued function of position.

Using the scalar potential to compute the vacuum field has several advantages. The scalar potential is described using a *single* function of position, namely $\tilde{\Phi}$, whereas the magnetic vector potential, $\mathbf{A} = A_\theta\nabla\theta + A_\phi\nabla\phi$, is described by *two* scalar functions of position, namely A_θ and A_ϕ (this is assuming that the gauge freedom is used to remove A_s). The constraints on the enclosed total plasma current, I, and the enclosed coil linking current, G, can be enforced directly and *exactly*. The "current" density, $\mathbf{j} \equiv \nabla\times\nabla\Phi$, is identically equal to zero, regardless of the numerical resolution.

However, using the scalar potential has disadvantages that stem from the inevitability of finite numerical accuracy. The divergence-free property of the magnetic field, $\nabla\cdot\mathbf{B} \equiv \nabla\cdot\nabla\Phi$, is not *exactly* equal to zero; and neither can the boundary conditions $\mathbf{B}\cdot\mathbf{x}_\theta\times\mathbf{x}_\phi = 0$ on the plasma boundary and $\mathbf{B}\cdot\mathbf{x}_\theta\times\mathbf{x}_\phi = B^n$ on the computational boundary be *exactly* enforced.

Algorithms for constructing the scalar potential for the field in the vacuum region have been implemented in SPEC , but the calculations presented herein employed the routines for representing the vacuum magnetic field as the curl of the magnetic vector potential. Future investigations will fully explore the advantages and disadvantages of both numerical representations.

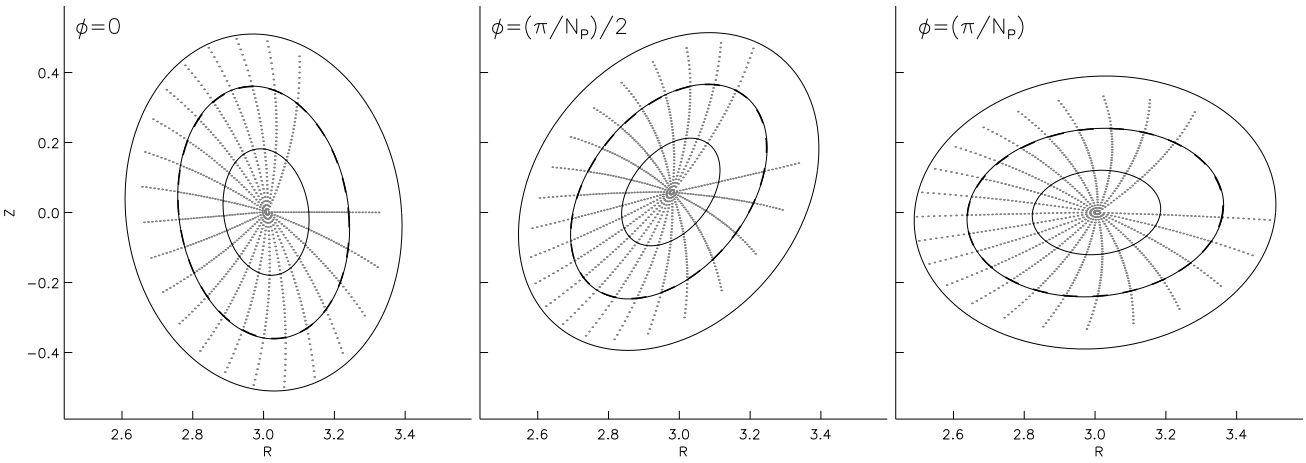

FIG. 1: A comparison between the Poincaré plots produced by using the magnetic field from a free-boundary SPEC "stellarator geometry" calculation and by using the magnetic field produced by the Biot-Savart law is shown. On this scale, the agreement is excellent. A quantitative comparison is shown in Fig. 2.

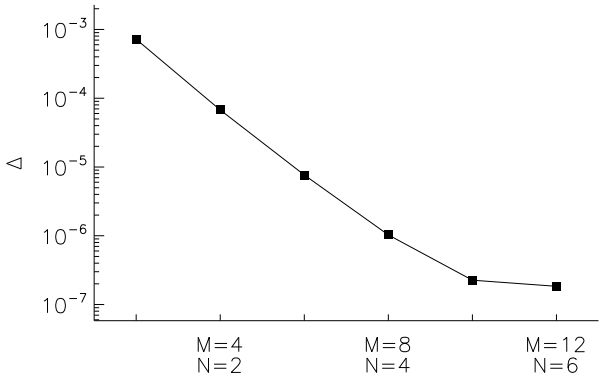

FIG. 2: Error between the SPEC magnetic field and the Biot-Savart field is plotted against Fourier resolution.

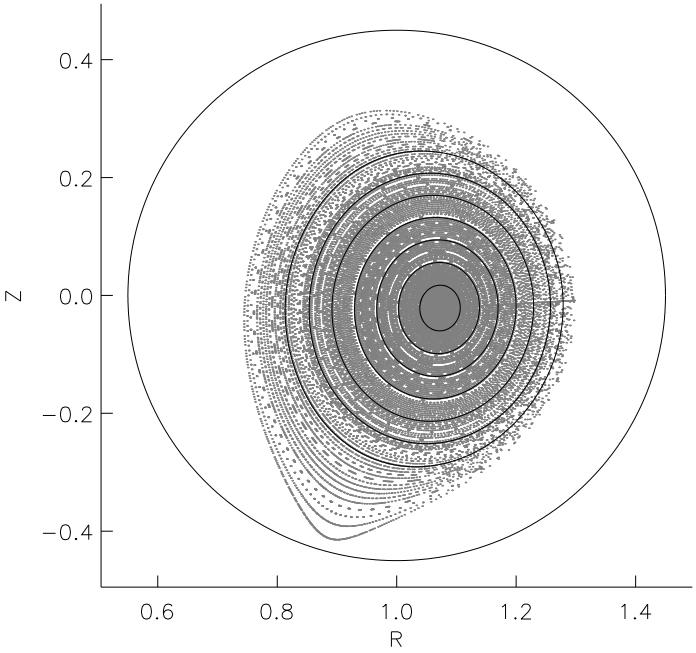

FIG. 3: Tokamak case.